ALUMINUM NITRIDE PIEZOELECTRIC MICROMACHINED ULTRASOUND TRANSDUCER ARRAYS

Stefon Shelton[1], Andre Guedes[1], Richard Przybyla[2], Reut Krigel[2], Bernhard Boser[2], David A. Horsley[1]
[1]Berkeley Sensor & Actuator Center, University of California, Davis, CA, USA
[2] Berkeley Sensor & Actuator Center, University of California, Berkeley, CA, USA

ABSTRACT

Air-coupled piezoelectric micromachined ultrasound transducer arrays, operating at ~190 kHz, have been fabricated utilizing an aluminum nitride piezoelectric layer. Improved fabrication processes have reduced the frequency variation seen in our previous work with single transducers resulting in arrays of transducers with resonant frequencies (f_n) that match within the fractional half-power bandwidth, 1/Q = 6.6%, of the transducer. Matching of $\Delta f/f < 2\%$ has been achieved across a 20 element 2-D array.

INTRODUCTION

Ultrasound transducers have many applications in medical imaging, ranging, robotics, and velocity sensing. Microelectromechanical systems (MEMS) micromachined ultrasound transducers (MUTs) have been explored for use in many of these applications and both capacitive and piezoelectric transduction methods have been demonstrated [1, 2].

The piezoelectric actuation we have chosen for use in our transducers offers several advantages over capacitive drive for in-air applications. In order to achieve the large displacement required for effective coupling to the air, cMUTs typically require large DC bias and drive voltages (>100V) [3]. Piezoelectric actuation requires much lower drive voltage (<15V) [4]. In addition, our pMUTs utilize a simple fabrication process and do not require tight control of the backside gap that is necessary for consistent cMUT performance.

Much of the previous work on pMUTs has focused on lead zirconate titanate (PZT) and zinc oxide (ZnO) piezoelectric materials [2, 5-7]. While PZT has higher piezoelectric constants [8] than the aluminum nitride (AlN) film used in this work, the lower dielectric constant of AlN allows for comparable performance to be achieved. In addition, AlN is deposited in a low-temperature (<400° C) sputtering process that is compatible with CMOS processes allowing for future integration with signal-processing electronics which is particularly attractive for phased-array applications.

In this work we focus on fabrication challenges and characterization of a well-matched 2D air-coupled AlN pMUT array operating in the 200 kHz region. In our previous work we have developed both ranging and distance sensing systems [4, 9] using single transducers [10, 11]. By fabricating a frequency-matched array we can extend the utility of these transducers by allowing them to be operated as a phased array, thereby increasing the output sound pressure and creating a narrow, steerable output beam. This allows us to extend our range-finding system to include both distance and angle to an object [12] allowing for simple gesture recognition applications.

TRANSDUCER DESIGN AND FABRICATION

The transducer, with cross section schematic shown in Fig. 1, is based on a piezoelectric unimorph membrane formed from a patterned SiO_2/AlN/Mo/AlN/Al layer stack deposited on a Si wafer.

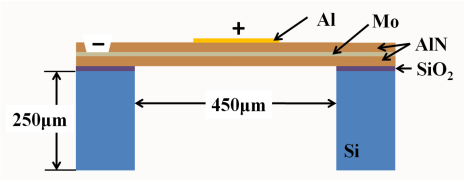

Figure 1: Cross section schematic of pMUT device.

The 450 µm diameter circular membrane is actuated by applying an excitation voltage between a 300 µm diameter top electrode and a continuous bottom electrode located at the transducer's mid-plane. The applied electric field creates a transverse stress in the active AlN layer which causes the membrane to displace out-of-plane producing a pressure wave in the air.

The transducer dimensions and operating parameters are shown in Table 1. The membrane diameter is chosen to produce the desired natural frequency (~200 kHz) for 1 µm thick AlN active and passive layers. Individually-addressed hexagonal 2-D arrays were fabricated with a center-to-center spacing of 0.9 mm or approximately λ/2 for a 190 kHz transducer. Fig. 2 shows an optical micrograph image of the individually-addressed 37 element hexagonal array on a 6.5 mm die.

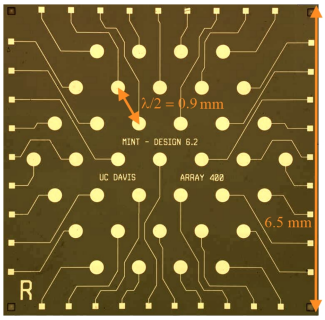

Figure 2: Optical image of a 37 element pMUT die measuring 6.5 mm square

Table 1: Transducer parameters

Parameter	Value	Units
Membrane thickness	2.1	µm
Membrane diameter	450	µm
Top electrode diameter	300	µm
Center-to-center spacing	900	µm
Natural frequency, f_n	190	kHz
Quality factor, Q	15	-

The fabrication process flow is shown in Fig. 3. Fabrication begins with the deposition of a 0.2 µm layer of SiO_2, after which the structural layers are deposited via sputtering: a 1 µm AlN passive layer, the 100 nm Mo bottom electrode, and the final 1 µm active AlN layer. The 200 nm thick Al top electrode is then deposited and patterned using a lift-off process, after which contacts to the bottom electrode are opened in the AlN using a MF-319 wet etch. The wafer is then thinned by grinding to a thickness of 250 µm and the backside is patterned and etched using a deep

reactive ion etch (DRIE), stopping on the thin 0.2 µm oxide layer. The oxide layer is removed using a separate plasma etch tool to obtain the final released membrane.

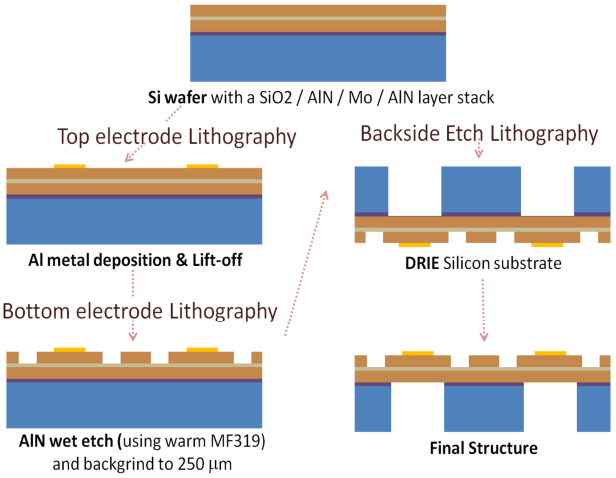

Figure 3: Fabrication process flow

EXPERIMENTAL RESULTS

a. Acoustic Testing

Acoustic tests were performed on packaged pMUT arrays using a burst measurement technique. The pMUT array is mounted in the center of a rotating stage and the acoustic axis is aligned with a microphone and is driven using a function generator with a 3.5 V_{rms}, 30 cycle burst at the natural frequency of the membranes. The burst is generated every 10 ms. The output signal from the microphone is amplified and band pass filtered, then the time domain signal is captured with an oscilloscope. A schematic of the test setup and a representative received burst is shown in Fig. 4. The relative output pressure is determined using the peak to peak value of the received burst.

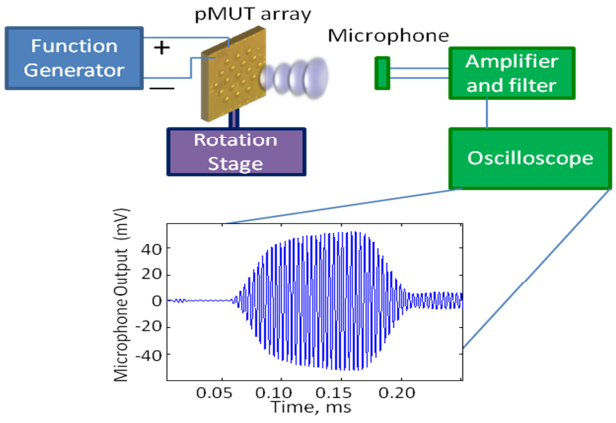

Figure 4: Acoustic test setup diagram and representative received burst

We first explored the relationship between the on-axis output sound pressure and the number of excited transducers. To do this we incremented the number of excited transducers (driven in parallel) and measured the relative output pressure at a fixed distance of 5.8 cm. Fig. 5 shows the results of the experiment for the 20 operative transducers in the array. The linear relation matches well with established acoustic theory [13].

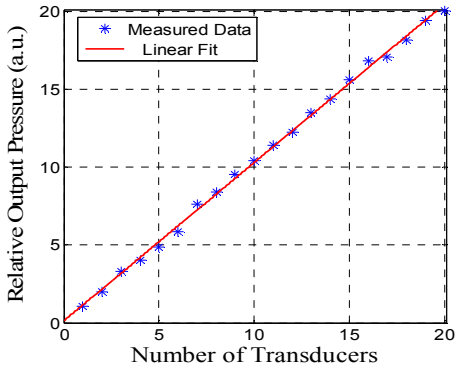

Figure 5: Sound pressure measured on-axis as a function of number of excited transducers, N. The sound pressure increases linearly with N.

The output pressure directivity pattern of the 20-transducer 2D array was measured using the previously described burst measurement setup and rotating the pMUT array relative to a single pMUT microphone. We scanned ±90° in both the X and Y axes and the result is shown in Fig. 6. As expected, we obtain a narrow main lobe with smaller side lobes. The width of the main lobe is 20° and agrees well with acoustic modeling.

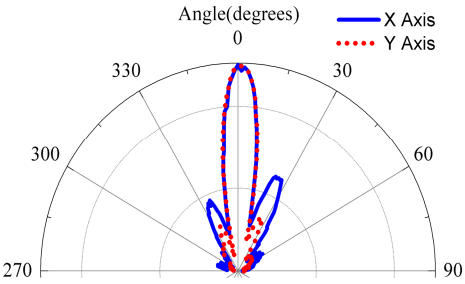

Figure 6: Output sound pressure directivity pattern for a 20-element 2D array.

Because sound is emitted from both the front and back sides of the array, the effect of backside reflections was explored using a variation of the burst measurement technique described previously. The microphone was placed at a distance of 1.5 cm from the front side of the membrane to measure the acoustic output while the distance between an acoustic reflector and the backside of the membrane was varied using a linear translation stage. The results are shown in Fig. 7.

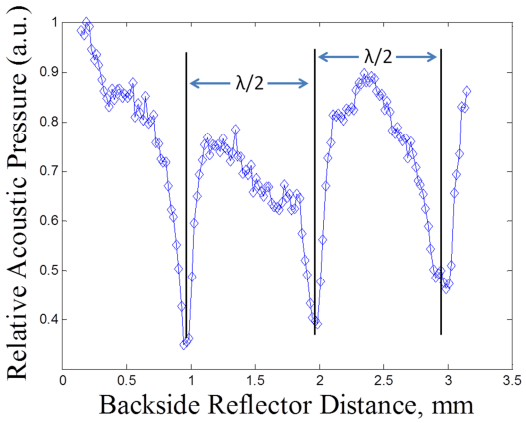

Figure 7: Output sound pressure from the front side of the membrane (normalized to the maximum) for varying distances to a backside acoustic reflector.

The reflector on the backside of the transducer causes a standing pressure wave to form between the reflector and the transducer. The acoustic output minima correspond with the nodes in the standing wave pattern and occur every λ/2 as predicted by acoustic theory.

b. Fabrication Variation

One of the challenges of fabricating pMUT arrays is ensuring that the pMUTs in the array have matching frequency responses. Our target matching metric is the transducer half-power bandwidth, 1/***Q***, which for our devices is 6.6%.

Across a single die, a main source of mismatch was geometric variation created by the backside DRIE process. Fig. 8 shows a cross-section SEM of a transducer prior to etch optimization and illustrates a 14 µm diameter variation due to undercut at the membrane edge. A 3-D FEM model in COMSOL (version 4.2a) predicts a 7% frequency mismatch for this level of variation. To quantify the frequency spread across a die we measured the frequency response of each transducer using a laser Doppler vibrometer (LDV). The frequency spread for a 17 element array prior to our process improvements is shown in Fig. 9 and illustrates matching of $\Delta f/f$ ~8% achieved with the early DRIE profile.

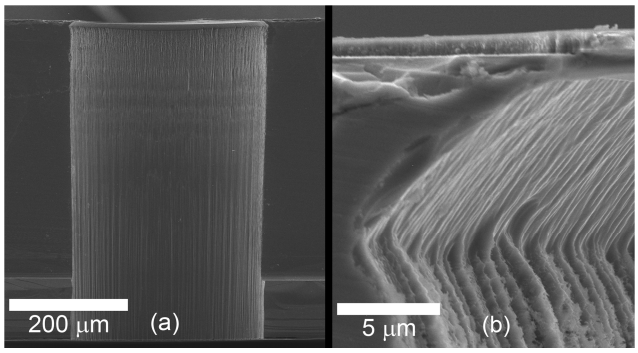

Figure 8: SEM images of pMUT cross-section prior to etch optimization: (a) profile (b) close up of membrane edge showing undesired undercut.

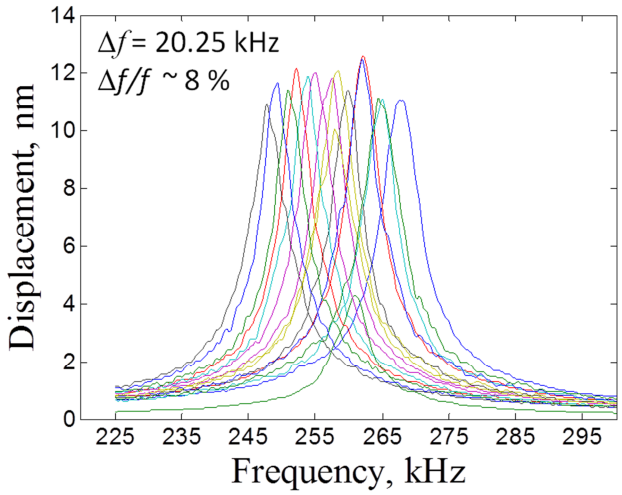

Figure 9: Frequency response of a 17 element array prior to etch optimization.

In order to correct this undercut we optimized the DRIE release step. In the standard DRIE process, the RF power is provided by a 13.56 MHz signal on the electrode (platen). To this process we added a low frequency generator at 380 kHz to bias the substrate platen during the etching cycle, allowing electrons to discharge the ion accumulation on the SiO_2 surface, reducing the notching effect. This leads to a more uniform etch profile which translates to less frequency variation across the die. Additionally we also observed better etch uniformity reducing the etch rate by decreasing the gases flow rates. Fig. 10 shows a cross-section of a pMUT etched with the optimized DRIE process in which the diameter variation has been reduced more than threefold to 4.2 µm. Additionally, as shown in Fig. 11, the frequency matching across an array has improved to $\Delta f/f$ < 2% which is well within the fractional half-power bandwidth (6.6%) requirement.

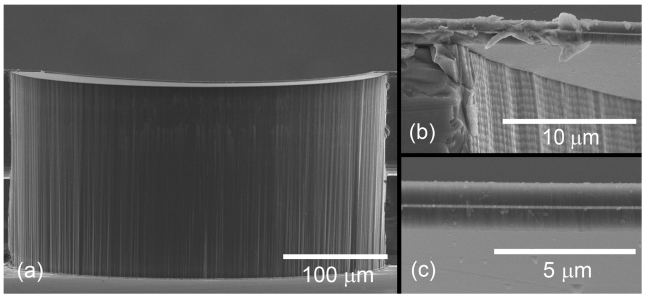

Figure 10: SEM images of pMUT after etch optimization and back-grinding: (a) profile (b) close up of membrane edge profile (c) pMUT cross-section showing well-aligned AlN layers.

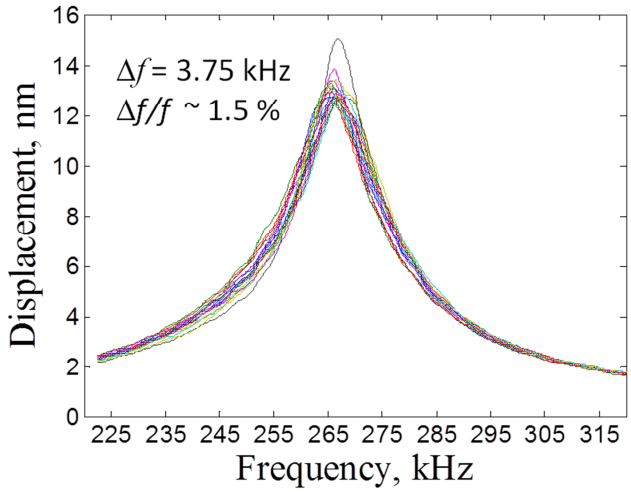

Figure 11: Frequency response of a 20 element array after etch optimization.

A second source of frequency mismatch is the across-wafer residual stress gradient. As the residual stress in the pMUT membrane becomes more tensile, the effective stiffness, and therefore the resonant frequency, increases. To quantify this effect, the frequency response was measured on 234 transducers distributed across a representative 150 mm wafer using the LDV. From this data we calculated the static displacement per volt and plotted the measured value as a function of the natural frequency, as shown in Fig. 12. The results are in good agreement with FEM predictions and show that the displacement diminishes approximately as f_n^{-2}.

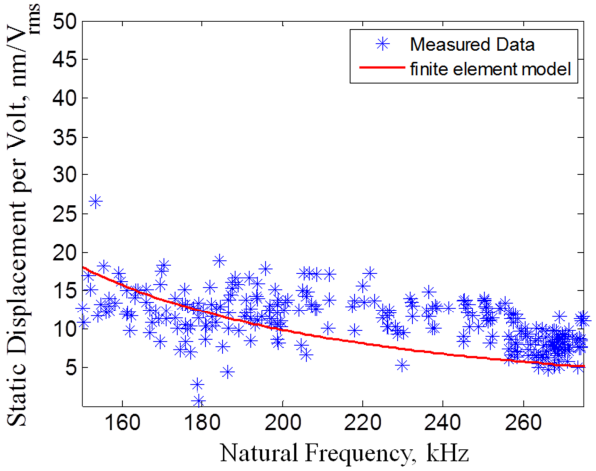

Figure 12: Static displacement per volt as a function of pMUT natural frequency, f_n.

From the measured frequency response the natural frequency (f_n) was determined and converted into a local stress estimate via a FEM model relating stress and f_n as shown in the inset of Fig. 13. Fig. 13 plots the predicted stress distribution across the wafer. Averaging these data points yields an average stress of –26.6 MPa, which matches the –25 MPa value measured in a thin-film stress measurement tool prior to fabrication.

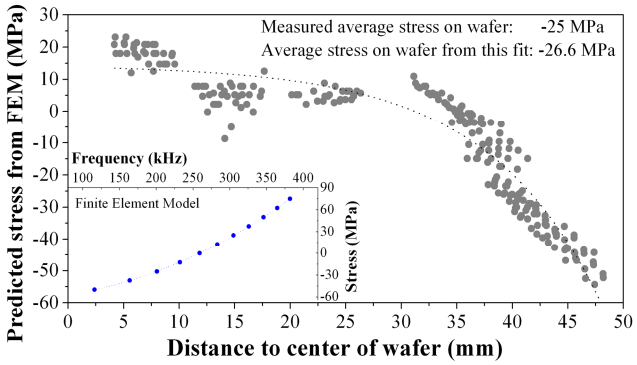

Figure 13: Across-wafer stress variation. Predicted stress was obtained from the measured natural frequency for 234 devices using the inset FEM model.

CONCLUSION

Air-coupled AlN pMUT arrays have been successfully fabricated using a simple CMOS compatible process. Recent improvements to the backside DRIE process have improved the frequency matching across a 20 transducer die to $\Delta f/f < 2\%$ allowing for improved performance relative to our previous single element transducers. An FEM model to predict the effect of residual stress on the frequency matching has been developed and the across wafer frequency variation due to stress shown. The relation between the number of driven transducers and the on-axis sound pressure level was found to be linear. The directivity of the 2-D array was determined and the main lobe width was found to be 20°.

ACKNOWLEDGMENT

This material is based upon work supported by the Defense Advanced Research Projects Agency (DARPA) and/or the Space and Naval Warfare Center, San Diego (SPAWAR SSC SD) under Contract No. N66001-08-C-2023.

REFERENCES

[1] I. O. Wygant, N. Jamal, H. Lee *et al.*, "An integrated circuit with transmit beamforming flip-chip bonded to a 2-D CMUT array for 3-D ultrasound imaging," *Ultrasonics, Ferroelectrics and Frequency Control, IEEE Transactions on,* vol. 56, no. 10, pp. 2145-2156, 2009.

[2] P. Muralt, N. Ledermann, J. Paborowski *et al.*, "Piezoelectric micromachined ultrasonic transducers based on PZT thin films," *Ultrasonics, Ferroelectrics and Frequency Control, IEEE Transactions on,* vol. 52, no. 12, pp. 2276-2288, 2005.

[3] I. O. Wygant, M. Kupnik, J. C. Windsor *et al.*, "50 kHz capacitive micromachined ultrasonic transducers for generation of highly directional sound with parametric arrays," *Ultrasonics, Ferroelectrics and Frequency Control, IEEE Transactions on,* vol. 56, no. 1, pp. 193-203, 2009.

[4] R. J. Przybyla, S. E. Shelton, A. Guedes *et al.*, "In-air rangefinding with an AlN piezoelectric micromachined ultrasound transducer," *Sensors Journal, IEEE,* vol. 11, no. 11, pp. 2690-2697, 2011.

[5] B. Belgacem, F. Calame, and P. Muralt, "5I-2 thick PZT sol-gel films for pMUT transducers performances improvement." pp. 926-929.

[6] F. Guo-Hua, C. S. Charles, Q. F. Zhou *et al.*, "Fabrication of MEMS ZnO dome-shaped-diaphragm transducers for high-frequency ultrasonic imaging," *Journal of Micromechanics and Microengineering,* vol. 15, no. 3, pp. 586, 2005.

[7] Y. Ito, K. Kushida, K. Sugawara *et al.*, "A 100-MHz ultrasonic transducer array using ZnO thin films," *Ultrasonics, Ferroelectrics and Frequency Control, IEEE Transactions on,* vol. 42, no. 2, pp. 316-324, 1995.

[8] S. Trolier-McKinstry, and P. Muralt, "Thin film piezoelectrics for MEMS," *Journal of Electroceramics,* vol. 12, no. 1, pp. 7-17, 2004.

[9] R. J. Przybyla, A. Flynn, V. Jain *et al.*, "A micromechanical ultrasonic distance sensor with >1 meter range," in Transducers, Bejing, China, 2011.

[10] S. Shelton, M.-L. Chan, H. Park *et al.*, "CMOS-Compatible AlN piezoelectric micromachined ultrasonic transducers," in IEEE International Ultrasonics Symposium (IUS), Rome, Italy, 2009, pp. 402-405.

[11] A. Guedes, S. Shelton, R. Przybyla *et al.*, "Aluminum nitride pMUT based on a flexurally-suspended membrane," in Transducers, Bejing, China, 2011.

[12] R. J. Przybyla, S. E. Shelton, A. Guedes *et al.*, "In-air ultrasonic rangefinding and angle estimation using an array of AlN micromachined transducers," in Hilton Head solid-State Sensors, Actuators, and Microsystems Workshop, Hilton Head, SC, June 2012.

[13] D. T. Blackstock, *Fundamentals of physical acoustics*: Wiley, 2000.

CONTACT

*S.E. Shelton, tel: +1-510-752-5180; seshelton@ucdavis.edu